Anisotropy-Induced Feshbach Resonances in a Quantum Dipolar Gas of Highly Magnetic Atoms

Alexander Petrov,[1,*] Eite Tiesinga,[2] and Svetlana Kotochigova[1,†]

[1]*Department of Physics, Temple University, Philadelphia, Pennsylvania 19122, USA and National Institute of Standards and Technology, Gaithersburg, Maryland 20899, USA*

[2]*Joint Quantum Institute, National Institute of Standards and Technology and University of Maryland, Gaithersburg, Maryland 20899, USA*

(Received 6 March 2012; published 7 September 2012)

We explore the anisotropic nature of Feshbach resonances in the collision between ultracold highly magnetic submerged-shell dysprosium atoms in their energetically lowest magnetic sublevel, which can only occur due to couplings to rotating bound states. This is in contrast to well-studied alkali-metal atom collisions, where broadest (strongest) Feshbach resonances are hyperfine induced and due to rotationless bound states. Our first-principle coupled-channel calculation of the collisions between these spin-polarized bosonic dysprosium atoms reveals a strong interplay between the anisotropies in the dispersion and magnetic dipole-dipole interaction. The former anisotropy is absent in alkali-metal and chromium collisions. We show that both types of anisotropy significantly affect the Feshbach spectrum as a function of an external magnetic field. Effects of the electrostatic quadrupole-quadrupole interaction are small. Over a 20 mT magnetic field range, we predict about 10 Feshbach resonances and show that the resonance locations depend on the dysprosium isotope.

DOI: 10.1103/PhysRevLett.109.103002 PACS numbers: 31.10.+z, 03.65.Nk, 34.50.−s

A strongly interacting quantum gas of highly magnetic atoms, placed in an optical lattice, provides the opportunity to examine strongly correlated matter, creating a platform to explore exotic many-body phases known in solids, quantum ferrofluids, quantum liquid crystals, and supersolids [1,2]. Recent experimental advances [3–10] in trapping and cooling magnetic atoms pave the way towards these goals.

In general, interactions between magnetic atoms are orientationally dependent or anisotropic. At room temperature, anisotropic interactions are much smaller than kinetic energies and other major interactions between atoms and, therefore, can be ignored. The situation is different for an ultracold gas of atoms with a large magnetic moment. For example, the anisotropy due to magnetic dipole-dipole interactions between ultracold chromium atoms leads to an anisotropic deformation of a Bose-Einstein condensate (BEC) [11]. Moreover, anisotropy plays a dominant role in collisional relaxation of ultracold atoms with large magnetic moments [5–7,12–15].

In this Letter, we pursue ideas for using anisotropic magnetic and dispersion interactions to control collisions of ultracold magnetic atoms by using Feshbach resonances [16]. Feshbach resonances make it possible to convert a weakly interacting gas of atoms into one that is strongly interacting and along the way promise to make available many of the collective many-body states mentioned above. Alternatively, interactions can be turned off altogether to create an ideal Fermi or Bose gas, for which thermodynamic properties are known analytically. Feshbach resonances can also be used to create BECs of weakly bound molecules [17], which can be optically stabilized to deeply bound molecules [18]. For fermionic atoms, the BCS-BEC phase transition [19] and universal many-body behavior of strongly interacting magnetic atoms can be studied via Feshbach resonances. Finally, three-body Efimov physics [20] can be explored.

The most promising atoms to study anisotropy in collisions are submerged-shell atoms, which have an electronic configuration with an unfilled inner shell shielded by a closed outer shell. In particular, we are interested in the rare-earth-metal dysprosium (Dy) atom with a $4f^{10}6s^2(^5I_8)$ ground state, a total angular momentum $j = 8$, and a large magnetic moment of $\approx 10\mu_B$. Its inner $4f^{10}$ shell electrons are spin aligned with an orbital angular momentum that is maximal and largely unquenched. Here, μ_B is the Bohr magneton. As a result, Dy's magnetic and dispersion properties are highly anisotropic. A quantitative description of the collision between two dysprosium atoms is challenging. For example, Ref. [15] showed that there are 153 Born-Oppenheimer (BO) potentials that dissociate to the ground $^5I_8 + {}^5I_8$ state.

We present a first-principle coupled-channel model allowing us to calculate anisotropy-induced magnetic Feshbach-resonance spectra of bosonic Dy atoms. The model treats the Zeeman, magnetic dipole-dipole, and isotropic and anisotropic dispersion interactions equally. Bosonic Dy isotopes have zero nuclear spin. Thus, there is no nuclear hyperfine structure and only Zeeman splittings remain. The weak quadrupole-quadrupole interaction [15] is included for completeness.

The focus of this Letter is on ultracold collisions of atoms prepared in the energetically lowest Zeeman state $j = 8$ and projection $m = -8$. Inelastic exothermic

atom-atom processes, where the spin projection of one or both of the atoms changes, are absent, and consequently, Feshbach resonances can be readily observed. In fact, in collisions with atoms in this "stretched" state there exists exactly one channel with zero relative nuclear orbital angular momentum $\vec{\ell}$. Consequently, for ultracold collisions resonances only occur due to anisotropic coupling to bound states with nonzero ℓ. This is in contrast with collisions between alkali-metal atoms in the energetically lowest hyperfine level. Multiple $\ell = 0$ or s-wave channels are present and s-wave Feshbach resonances exist.

We start by setting up the Hamiltonian, interatomic potentials, and channel basis for two bosonic $^5I_8$ Dy atoms with zero nuclear spin. This Hamiltonian assuming a magnetic field B along the $\hat{z}$ direction is

$$H = -\frac{\hbar^2}{2\mu_r}\frac{d^2}{dR^2} + \frac{\vec{\ell}^2}{2\mu_r R^2} + H_Z + V(\vec{R}, \tau), \qquad (1)$$

where $\vec{R}$ describes the orientation of and separation between the two atoms. The first two terms are the radial kinetic and rotational energy operators, respectively. The Zeeman interaction is $H_Z = g_j \mu_B (j_{1z} + j_{2z})B$ with $g_j = 1.24159$ the g factor of Dy [21], and j_{iz} is the z component of the angular momentum operator $\vec{j}_i$ of atom $i = 1, 2$. The electronic Hamiltonian, including nuclear repulsion, $V(\vec{R}, \tau)$ is anisotropic, and τ labels the electronic variables. Finally, μ_r is the reduced mass, and for $R \to \infty$ the interaction $V(\vec{R}, \tau) \to 0$.

Our coupled-channel calculations [22] are performed in the atomic basis $|(j_1 j_2) j m_j, \ell m_\ell\rangle \equiv Y_{\ell m_\ell}(\theta, \phi)|(j_1 j_2) j m_j\rangle$, where $\vec{j} = \vec{j}_1 + \vec{j}_2$ with its projection m_j, $Y_{\ell m_\ell}(\theta, \phi)$ is a spherical harmonic and angles θ and ϕ give the orientation of the internuclear axis relative to the magnetic field direction. In this basis, the Zeeman and rotational interaction are diagonal with energies $g_j \mu_B m_j B + \hbar^2 \ell(\ell+1)/(2\mu_r R^2)$. Coupling between the basis states is due to $V(\vec{R}, \tau)$ and will be discussed in detail below. Excited atomic states, for example those with $j_i \neq 8$, are not included as their internal energy is sufficiently high that the effects of coupling to these states is negligible. The Hamiltonian H conserves $M_{\rm tot} = m_j + m_\ell$ and is invariant under the parity operation so that only even (odd) ℓ are coupled. For homonuclear collisions, only basis states with even $j + \ell$ exist. Figure 1 shows an example of the long-range diagonal matrix elements in the atomic basis of the sum of the rotational, Zeeman, and electronic Hamiltonian. We have used $M_{\rm tot} = -16$ and even $\ell \leq 10$. In fact, only the potentials dissociating to the six energetically lowest Zeeman states are shown. The large number of potentials indicates the large number of resonances that, in principle, are possible.

Coupling between basis states is due to $V(\vec{R}, \tau)$. It is convenient to first evaluate this operator in a molecular basis with body-fixed projection quantum numbers defined

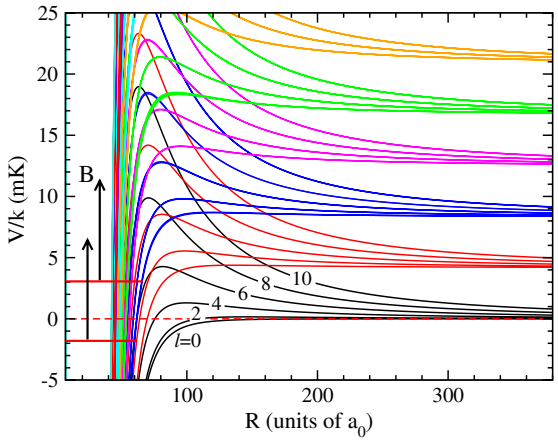

FIG. 1 (color online). Potential energy curves for ^{164}Dy + ^{164}Dy collisions in a magnetic field B as a function of internuclear separation. The (red) dashed line with zero energy indicates the energy of the entrance channel. A resonance occurs when a bound state energy equals the entrance-channel energy. The graph shows the 91 diagonal potential matrix elements at $B = 50$ G for channels $|(j_1 j_2) j m_j, \ell m_\ell\rangle$ with $m_j + m_\ell = -16$ and even $\ell \leq 10$. The curves are colored by their m_j value. The ℓ value for $m_j = -16$ curves is indicated. Here 1 G = 0.1 mT, $a_0 = 0.0529177$ nm is the Bohr radius, and $k = 1.38065 \times 10^{-23}$ J/K is the Boltzmann constant.

with respect to the internuclear axis. We use the molecular basis $|(j_1 j_2) j \Omega\rangle$ with projection Ω of $\vec{j}$ along the internuclear axis. The matrix elements of $V(\vec{R}, \tau)$ conserve the projection Ω but not j. The eigenenergies of $V(\vec{R}, \tau)$ at each value of R are the adiabatic (relativistic) BO potentials [23,24]. Typically, these potentials $U_{n|\Omega|\sigma}(R)$ are obtained from an electronic structure calculation and labeled by $n|\Omega|^{\pm}_{\sigma}$, where $|\Omega|$ is the absolute value of Ω, $\sigma = g/u$ is the gerade/ungerade symmetry of the electronic wave function, and $n = 1, 2, \ldots$ labels curves of the same $|\Omega|^{\pm}_{g/u}$ in order of increasing energy. For bosonic Dy_2, the 81 gerade (72 ungerade) states are superpositions of even (odd) j.

For $R > 27a_0$, beyond the Le Roy radius where the atomic electron clouds have negligible overlap, $V(\vec{R}, \tau)$ is the sum of the magnetic dipole-dipole, $V_{\mu\mu}(\vec{R}) \propto 1/R^3$, the electrostatic quadrupole-quadrupole, $V_{QQ}(\vec{R}) \propto 1/R^5$, and the van der Waals dispersion $V_{\rm disp}(\vec{R}) \propto 1/R^6$ interaction. Reference [15] reported the matrix elements of the operator $V_{\rm disp}(\vec{R})$ in the molecular basis and tabulated the adiabatic $C_{6,n\Omega\sigma}$ dispersion coefficients obtained by diagonalizing $V_{\rm disp}(\vec{R})$. Crucially, the eigenfunctions of $V_{\rm disp}(\vec{R})$ are independent of R.

At shorter range, coupling between basis states is more complex. Rather than determining all BO potentials, we have opted for the following approach. First, we calculate the single gerade potential $U_{16g}(R)$ with maximal projection $\Omega = 16$ (and omitting the $n = 1$ label) using a

coupled-cluster method with single, double, and perturbative triple excitations [CCSD(T)] [25] together with the scalar relativistic Stuttgart ECP28MWB pseudopotential and associated atomic basis sets $(14s, 13p, 10d, 8f, 6g)/[10s8p5d4f3g]$. The potential has a minimum at $R_e = 8.771a_0$ with depth $D_e/(hc) = 785.7\ \mathrm{cm}^{-1}$. For $^{164}\mathrm{Dy}_2$, it has a $\omega_e/(hc) = 25.6\ \mathrm{cm}^{-1}$ and has 71 bound states.

We then assume that the $R < 27a_0$ electronic wave functions of the adiabatic BO potentials are the same as those determined by the dispersion interaction, and the relation between energies of the *ab initio* potentials is the same as for its C_6 coefficient. I.e., for $R < 27a_0$ the adiabatic potentials satisfy $U_{n\Omega\sigma}(R)/U_{n'\Omega\sigma}(R) = C_{6,n\Omega\sigma}/C_{6,n'\Omega'\sigma}$ with the R-independent eigenfunctions of the dispersion interaction. As an initial model of the short-range interactions this approach is justified because at $R = 27a_0$ the dispersion potential is the dominant interaction. Furthermore, the open $4f^{10}$ shell is located deep within the core, does not overlap significantly with the electron cloud of the nearby Dy atom, and thus for $R < 27a_0$, does not induce significant additional anisotropic interactions. Bonding is predominantly due to overlap of the isotropic $6s^2$ shells.

Equivalently, $V(\vec{R}, \tau)$ is given by

$$V(\vec{R}, \tau) = V_{\mu\mu}(\vec{R}) + V_{QQ}(\vec{R}) + \frac{U_{16g}(R)}{U_{LR,16g}(R)} V_{\mathrm{disp}}(\vec{R}) \qquad (2)$$

for any R, where $U_{LR,16g}(R)$ is the long-range form of the $\Omega = 16$ BO potential. Hence, $U_{16g}(R) = U_{LR,16g}(R)$ for $R > 27a_0$ where it contains contributions from the dispersion and quadrupole-quadrupole interaction. Most importantly, Eq. (2) shows that there is only one independent short-range potential.

For practical reasons, it is advantageous to write $V_{\mathrm{disp}}(\vec{R})$ as a sum of spherical tensor operators in the laboratory frame. That is

$$V_{\mathrm{disp}}(\vec{R}) = \frac{1}{R^6} \sum_{kq} \sum_{i} c_k^{(i)} (-1)^q C_{k,-q}(\theta, \phi) T_{kq}^{(i)}, \qquad (3)$$

where $C_{kq}(\theta, \phi) = \sqrt{4\pi/(2k+1)} Y_{kq}(\theta, \phi)$ and the spherical tensors $T_{kq}^{(i)}$ of rank k and with components q are defined by

$$\begin{aligned}
&T_{00}^{(1)} = I, \qquad T_{2q}^{(1)} = [j_1 \otimes j_1]_{2q} + [j_2 \otimes j_2]_{2q}, \\
&T_{2q}^{(2)} = [j_1 \otimes j_2]_{2q}, \qquad T_{00}^{(2)} = [j_1 \otimes j_2]_{00}, \\
&T_{4q}^{(1)} = [[j_1 \otimes j_1]_2 \otimes [j_2 \otimes j_2]_2]_{4q}, \\
&T_{2q}^{(3)} = [[j_1 \otimes j_1]_2 \otimes [j_2 \otimes j_2]_2]_{2q}, \\
&T_{00}^{(3)} = [[j_1 \otimes j_1]_2 \otimes [j_2 \otimes j_2]_2]_{00}, \qquad (4)
\end{aligned}$$

where I is the identity operator and $[j \otimes j']_{kq}$ denotes a tensor product of angular momentum operators $\vec{j}$ and $\vec{j}'$ coupled to an operator of rank k and component q [26]. The higher-order tensor operators are constructed in an analogous manner. Equation (4) has three, three, and one tensors $T_{kq}^{(i)}$ of rank $k = 0$, 2, and 4, respectively. The seven dispersion coefficients $c_k^{(i)}$ are listed in Table I. The operator order in Eq. (4) is by decreasing absolute value of $c_k^{(i)}$. The isotropic $T_{00}^{(1)}$ term is the largest by far with the strongest anisotropic contribution from the dipolar operator $T_{2q}^{(1)}$ constructed from the angular momentum of only one atom coupled to the rotation of the molecule. Finally, the magnetic dipole-dipole and quadrupole-quadrupole interactions are

$$V_{\mu\mu}(\vec{R}) = \frac{1}{R^3} c_{\mu\mu} \sum_q (-1)^q C_{2,-q}(\theta, \phi) T_{2q}^{(2)} \qquad (5)$$

and

$$V_{QQ}(\vec{R}) = \frac{1}{R^5} c_{QQ} \sum_q (-1)^q C_{4,-q}(\theta, \phi) T_{4q}^{(1)}, \qquad (6)$$

respectively. Their strengths are listed in Table I.

Figure 2 shows the scattering length as a function of the magnetic field strength for the collision between two $m = -8$ ^{164}Dy atoms at a collision energy of $E/k = 30$ nK. We use $M_{\mathrm{tot}} = -16$ and include 91 channels with even $\ell \leq 10$. Fields up to $B = 200$ G are experimentally easily accessible [16]. The graph shows about 10 Feshbach resonances; some are broad, many are very narrow. By performing calculations that include fewer partial waves we have observed that the resonances can not be labeled by a single partial wave. For example, the broad resonances at $B \approx 30$, 110, and 170 G are already present when only $\ell = 0$, 2, and 4 channels are included. Their locations, however, shift significantly when higher ℓ channels are included and only converge to within a few Gauss when $\ell = 8$ channels are included. In general, we find that the magnetic-field location of a resonance that appears when channels with partial wave ℓ are included stabilizes when channels up to $\ell + 4$ are included. Hence, resonances can be labeled by the first partial wave quantum number for which the resonance appeared. In Fig. 2, the first partial wave for the three broad resonances is shown. We stress that this behavior with increasing number of partial waves is unlike that observed in alkali-metal atom collisions [16] or even in collisions of strongly magnetic chromium atoms

TABLE I. Dispersion coefficients $c_k^{(i)}$ in units of $E_H a_0^6$, where $E_H = 4.35974 \times 10^{-18}$ J is the Hartree energy. The strength of the magnetic dipole-dipole and quadrupole-qudrupole interactions are $c_{\mu\mu} = -5.0269 \times 10^{-3}\ E_H a_0^3$ and $c_{QQ} = 9.5719 \times 10^{-8}\ E_H a_0^5$, respectively.

$k \backslash i$	1	2	3
0	-1873.4	3.57×10^{-3}	-6.82×10^{-6}
2	-0.1680	5.06×10^{-3}	-8.15×10^{-6}
4	-6.56×10^{-5}		

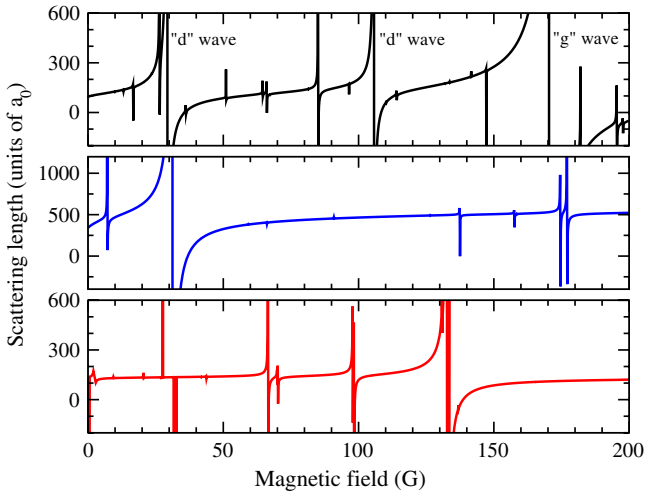

FIG. 2 (color online). Scattering length of $m = -8$ ^{164}Dy atoms as a function of magnetic field with and without the magnetic dipole-dipole or the anisotropic contribution of the dispersion interaction. We use a collision energy of $E/k =$ 30 nK. Channels with even partial waves ℓ up to 10 are included. The top panel shows the case when all interactions are included. At $B = 0$ the scattering length is $89a_0$. For the three broad resonances the first partial wave for which the resonance appears is shown. The middle and bottom panels are obtained when the dispersion and magnetic dipole-dipole anisotropy is set to zero, respectively.

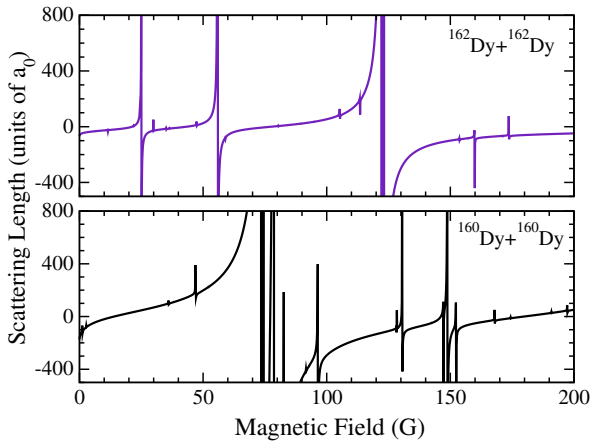

FIG. 3 (color online). Scattering length as a function of magnetic field for the bosonic isotopes ^{162}Dy (top panel) and ^{160}Dy (bottom panel). The initial state and number of included ℓ as in Fig. 2.

[27]. For these atoms, resonances do not shift by more than a few Gauss when additional partial waves are added. For dysprosium, the anisotropic interactions are so strong that states with different partial waves are strongly mixed.

We have also studied the effect of the uncertainty in the depth of $U_{16g}(R)$. The depth D_e was changed by adding a localized correction that does not modify the long-range potential. A depth change by ≈ 10 cm^{-1} changes its number of bound states by one. Even much smaller changes modify the resonance spectrum nontrivially. Resonance widths are dramatically modified and broad resonances that appear when d-wave channels are included can be observed.

The precise form of short-range potential and dispersion coefficients are not known. A few percent uncertainty is not unrealistic. For this Letter, we have constructed potentials that lead to a positive $B = 0$ scattering length a for ^{164}Dy atoms in the $m = -8$ state. This choice is suggested by a recent observation of a BEC of ^{164}Dy atoms at nearly zero magnetic field, which indicates a positive scattering length at this field [8]. Moreover, we chose the scattering length to be approximately equal to the mean scattering length [28] for a (fictitious) van der Waals potential with a C_6 coefficient equal to the isotropic dispersion coefficient.

To further elucidate the effect of anisotropy, Fig. 2 also shows the scattering length as a function of magnetic field when parts of the anisotropy are turned off. The top panel displays the case when all interactions are included. The bottom two panels show the effect of turning of the anisotropy in the dispersion and magnetic dipole-dipole interaction, respectively. The resonance spectra in the three panels are quite distinct. The number of resonances differs, and with one exception, the resonances are narrower.

Finally, Fig. 3 illustrates the effect of changing to different bosonic Dy isotopes. Since to good approximation BO potentials are indendent of isotope, the coupled-channels equations are solved using the appropriate reduced mass. This observation has explained the relationships between scattering lengths of isotopic combinations of spinless ytterbium [29], while its limitations for lithium Feshbach resonances have been studied in Ref. [30]. The field dependence of the scattering length for ^{160}Dy and ^{162}Dy are significantly different, indicating that measurement of resonance locations in different isotopes is invaluable in understanding Dy scattering.

Conclusion.—Applying a full coupled-channels calculation for ultracold atom-atom collisions, we have shown that the origin of Feshbach resonances in interactions between ultracold rare-earth-metal atoms with large magnetic moments result from strong scattering anisotropies. By tuning an applied magnetic field, we predict resonances and control of collision cross sections even for atoms with zero nuclear spin. We have investigated the effects of different short- and long-range anisotropic potentials as well as different isotopes on the scattering length of Dy.

For a more realistic description of dysprosium collision we expect that the number of short-range parameters is larger than one. We observed that there are seven $c_k^{(i)}$ coefficients in Eq. (3) and Table I describing the long-range behaviour of all 153 BO potentials. Based on the nature of the submerged f^{10} shell, it is a reasonable assumption that we only need one short-range parameter for each of the seven $c_k^{(i)}$ coefficients. Furthermore, we note that not all

parameters might be equally important. For example, the relative strength of the $c_k^{(i)}$ coefficients shows that, at least at long range, some tensor operators are less relevant. We can use this observation to systematically increase the number of independent short-range parameters. This can only be validated by comparison to future experimental data.

This study forms a first prediction of the anisotropic nature of Feshbach resonances for ultracold dysprosium atoms. The specific positions of the resonances can not be predicted at this time due to the uncertainties in the short-range form of the interaction potentials. To optimize the potentials we must await experimental observations of resonances from multiple isotopic combinations.

We acknowledge support from grants of the AFOSR, NSF, and ARO.

*Also at St. Petersburg Nuclear Physics Institute, Gatchina, 188300, Russia; Division of Quantum Mechanics, St. Petersburg State University, 198904, Russia.

†Corresponding author.
skotoch@temple.edu

[1] B. M. Fregoso and E. Fradkin, Phys. Rev. Lett. **103**, 205301 (2009); B. M. Fregoso and E. Fradkin, Phys. Rev. B **81**, 214443 (2010).
[2] B. M. Fregoso, K. Sun, E. Fradkin, and B. L. Lev, New J. Phys. **11**, 103003 (2009).
[3] L. Santos and T. Pfau, Phys. Rev. Lett. **96**, 190404 (2006).
[4] J. J. McClelland and J. L. Hanssen, Phys. Rev. Lett. **96**, 143005 (2006).
[5] C. B. Connolly, Y. S. Au, S. C. Doret, W. Ketterle, and J. M. Doyle, Phys. Rev. A **81**, 010702(R) (2010).
[6] M.-J. Lu, V. Singh, and J. D. Weinstein, Phys. Rev. A **79**, 050702(R) (2009).
[7] M. Lu, S. H. Youn, and B. L. Lev, Phys. Rev. Lett. **104**, 063001 (2010).
[8] M. Lu, N. Q. Burdick, S. H. Youn, and B. L. Lev, Phys. Rev. Lett. **107**, 190401 (2011).
[9] D. Sukachev, A. Sokolov, K. Chebakov, A. Akimov, S. Kanorsky, N. Kolachevsky, and V. Sorokin, Phys. Rev. A **82**, 011405(R) (2010).
[10] M. Lu, N. Q. Burdick, and B. L. Lev, Phys. Rev. Lett. **108**, 215301 (2012).
[11] J. Stuhler, A. Griesmaier, T. Koch, M. Fattori, T. Pfau, S. Giovanazzi, P. Pedri, and L. Santos, Phys. Rev. Lett. **95**, 150406 (2005).
[12] S. Hensler, J. Werner, A. Griesmaier, P. O. Schmidt, A. Görlitz, T. Pfau, S. Giovanazzi, and K. Rzazewski, Appl. Phys. B **77**, 765 (2003).
[13] C. I. Hancox, S. C. Doret, M. T. Hummon, L. Luo, and J. Doyle, Nature (London) **431**, 281 (2004).
[14] R. V. Krems, G. C. Groenenboom, and A. Dalgarno, J. Phys. Chem. A **108**, 8941 (2004).
[15] S. Kotochigova and A. Petrov, Phys. Chem. Chem. Phys. **13**, 19165 (2011).
[16] C. Chin, R. Grimm, P. Julienne, and E. Tiesinga, Rev. Mod. Phys. **82**, 1225 (2010).
[17] T. Köhler, K. Góral, and P. S. Julienne, Rev. Mod. Phys. **78**, 1311 (2006).
[18] K.-K. Ni, S. Ospelkaus, M. H. G. de Miranda, A. Peér, B. Neyenhuis, J. J. Zirbel, S. Kotochigova, P. S. Julienne, D. S. Jin, and J. Ye, Science **322**, 231 (2008).
[19] S. Giorgini, L. P. Pitaevskii, and S. Stringari, Rev. Mod. Phys. **80**, 1215 (2008); I. Bloch, J. Dalibard, and W. Zwerger, Rev. Mod. Phys. **80**, 885 (2008).
[20] T. Kraemer, M. Mark, P. Waldburger, J. G. Danzl, C. Chin, B. Engeser, A. D. Lange, P. Pilch, A. Jaakkola, H.-C. Nägerl, and R. Grimm, Nature (London) **440**, 315 (2006).
[21] Yu. Ralchenko, A. E. Kramida, J. Reader, and NIST ASD Team, NIST Atomic Spectra Database, http://physics.nist.gov/asd (2011).
[22] A close-coupling calculation is a numerical method to find scattering solutions of a finite set of coupled radial Schrödinger equations.
[23] G. Herzberg, *Spectra of Diatomic Molecules* (D. Van Nostrand Company, New York, 1950).
[24] H. Lefebvre-Brion and R. W. Field, *Perturbations in the Spectra of Diatomic Molecules* (Academic Press, Inc., London, 1986).
[25] J. D. Watts, J. Gauss, and R. J. Bartlett, J. Chem. Phys. **98**, 8718 (1993).
[26] R. Santra and C. H. Greene, Phys. Rev. A **67**, 062713 (2003).
[27] J. Werner, A. Griesmaier, S. Hensler, J. Stuhler, T. Pfau, A. Simoni, and E. Tiesinga, Phys. Rev. Lett. **94**, 183201 (2005).
[28] G. F. Gribakin and V. V. Flambaum, Phys. Rev. A **48**, 546 (1993).
[29] M. Kitagawa, K. Enomoto, K. Kasa, Y. Takahashi, R. Ciuryło, P. Naidon, and P. S. Julienne, Phys. Rev. A **77**, 012719 (2008).
[30] E. Tiemann, H. Knöckel, P. Kowalczyk, W. Jastrzebski, A. Pashov, H. Salami, and A. J. Ross, Phys. Rev. A **79**, 042716 (2009).